



# Effect of Chemical Composition on the Microstructure and Properties of the Ag-Ga-Ge Alloys

Aleksandar Marković, Milena Premović, Duško Minić, Dejan Gurešić, Dragan Manasijević, and Aleksandar Djordjevic

(Submitted December 3, 2018; in revised form April 21, 2019; published online May 28, 2019)

This study presents a comparison of thermodynamically calculated phase compositions of Ag-Ga-Ge alloys at fixed temperatures with phase analysis results of alloys annealed at respective temperatures. Three isothermal sections of the Ag-Ga-Ge system at 25, 100 and 300 °C have been extrapolated using optimized thermodynamic parameters from the literature. An experimental analysis of the microstructure was carried out using optical microscopy, scanning electron microscopy and energy-dispersive spectrometry. Results obtained by x-ray powder diffraction methods (identified phases and lattice parameters) were compared with the results of the predicted phase equilibria. Good overall agreement between experimental and calculated values was obtained. The Brinell hardness and electrical conductivity of selected alloys were measured and obtained results were analyzed with respect to their overall compositions and phase constituents.

**Keywords** electrical conductivity, hardness, phase equilibrium, ternary Ag-Ge-Ga system

## 1. Introduction

The ternary Ag-Ge-Ga system has been investigated previously by our group (Ref 1). In our previous study, reliable thermodynamic dataset has been proposed (Ref 2-4) and experimentally confirmed with experimental investigation of 36 alloys from three vertical sections (Ag-GeGa, Ge-AgGa and Ga-AgGe) and two isothermal sections at 200 and 400 °C. Since reliable thermodynamic dataset has been obtained by previous study (Ref 1), in the current study, same thermodynamic parameters have been used for calculations of the three isothermal sections at 25, 100 and 300 °C. Thermodynamic calculations of the isothermal sections were performed by using PANDAT software (Ref 5). Calculated phase diagrams of the isothermal sections were compared with experimental results obtained in the current study. Experimental results were obtained by using scanning electron microscopy (SEM) with energy-dispersive spectrometry (EDS), x-ray powder diffraction (XRD) analysis and inverted metallographic microscope. Besides checking of the phase equilibrium, some of the important properties such as hardness and electrical conductivity were tested in the current study. Reason for testing these properties is due to contribution to further development of application area since Ag-Ge-based alloys have applications in the electronic industry (Ref 6-8). It is well known that silver and silver alloys represent excellent heat and electricity

conductors. Germanium-based alloys are extensively studied because of their semiconducting properties and special application in the modern technology for making optical disks, Blu-ray disks, flash memories, DVD, etc. (Ref 9-11). Due to the significant application of these alloys, understanding their properties is a matter of high importance. Obtained results presented in this study should benefit to the industry because they can be used as the basis for designing and developing new alloys.

## 2. Materials and Methods

High-purity (99.999 wt.%) Ag, Ga and Ge metals produced by Alfa Aesar (Germany) were used for preparation of investigated alloy samples. Total mass of each sample was 3 g. Weighed masses of the samples were arc-melted and re-melted five times under a high-purity argon atmosphere using a non-consumable tungsten electrode. The average weight loss of the samples during melting was about 1 mass%. After melting, samples were divided into three series (first series annealed at 300 °C, second series annealed at 100 °C and third series for electrical conductivity and hardness measurements). Samples for investigation of isothermal sections at 300 °C and 100 °C were sealed in evacuated quartz tubes and then heated to a temperature that is 50 °C higher than the melting temperature of Ag. The alloy samples were then cooled down to 300 °C (first series) and 100 °C (second series) at the cooling rate of 5 °C min<sup>-1</sup>. The samples were kept at 300 °C for four weeks and six weeks at 100 °C and then quenched in the water and ice mixture to preserve desired equilibrium at 300 and 100 °C. Those samples were prepared and used for SEM-EDS and XRD analysis. The compositions of the alloy samples were determined using a JEOL JSM-6460 scanning electron microscope (SEM) and TESCAN VEGA3 scanning electron microscope, which were both equipped with an EDS system (Oxford Instruments X-act). The samples for SEM-EDS analysis were first ground using sand paper, polished with diamond paste, and then cleaned in an ultrasonic bath. The overall compositions of

Aleksandar Marković, Milena Premović, Duško Minić, Dejan Gurešić, and Aleksandar Djordjevic, Faculty of Technical Science, University of Priština, Kneza Miloša 7, Mitrovica, Kosovo 28320, Serbia; and Dragan Manasijević, Technical Faculty in Bor, University of Belgrade, VJ 12, Bor 19210, Serbia. Contact e-mail: milena.premovic@gmail.com.

the annealed samples were determined by mapping the entire polished surfaces of the samples. By contrast, the compositions of the observed coexisting phases were determined examining the surface of the same phase at different parts of the sample (at least five different positions of the same phase were examined per phase). The chemical compositions of the phases determined in this study represented the mean values based on at least five individual analyses. Powder XRD data for the phase analysis of the alloy samples were recorded with a D2 PHASER (Bruker, Karlsruhe, Germany) powder diffractometer equipped with a dynamic scintillation detector and ceramic x-ray Cu tube (KFL-Cu-2K) in the  $2\theta$  range from  $10^\circ$  to  $75^\circ$  with a step size of  $0.02^\circ$ . Before the XRD analysis, the selected samples were first powdered using ball mill (YKT-04 machine) and the powders obtained were then placed in special holders and pressed to obtain compact samples. The recorded XRD patterns were subsequently analyzed using TOPAS 4.2 software and the International Centre for Diffraction Data (ICDD) Powder Diffraction Files (PDF2) database (2013). The lattice parameters were determined using TOPAS software and by performing full Rietveld refinement.

Third group of samples were used for light optical microscopy, XRD analysis, electrical conductivity and hardness measurements. These samples were again melted in an electric furnace under high-purity argon atmosphere and slowly cooled to the room temperature using a cooling rate of  $2^\circ\text{C min}^{-1}$  in a way to achieve equilibrium at room temperature for the hardness and electrical conductivity measurements. Obtained microstructure has been checked with XRD analysis. Samples were prepared by classic metallographic procedure without etching and sealed in the polymer. Samples are positioned in way to two dimensions were much greater than the third in way to have a large surface area which will be used for tests. Microstructures of the samples were recorded on a light microscopy using (LOM) OLYMPUS GX41 inverted metallographic microscope. Electrical conductivity measurements were carried out using Foerster SIGMATEST 2.069 eddy instrument. Hardness of the samples was measured using Brinell hardness tester INNOVATEST, model NEXUS 3001.

### 3. Results and Discussion

According to the previous study (Ref 1) and information about binary systems (Ref 2-4) in the ternary Ag-Ge-Ga system, seven phases should appear. One is liquid phase (L) and six solid phases [(Ag), (Ge), (Ga) solution phases and  $\zeta$ -Ag<sub>2</sub>Ga,  $\zeta'$ -Ag<sub>2</sub>Ga, Ag<sub>3</sub>Ga<sub>2</sub> intermetallic phases]. List of solid phases with their crystallographic data is given in Table 1.

**Table 1 Crystallographic information of the solid phases of the Ag-Ga-Ge system**

Thermodynamic database name	Phase	Pearson symbol	Space group	Lattice parameters, Å			References
				<i>a</i>	<i>b</i>	<i>c</i>	
FCC_A1	(Ag)	<i>cF4</i>	<i>Fm<math>\bar{3}</math>m</i>	4.0861			Ref 12
DIAMOND_A4	(Ge)	<i>cF8</i>	<i>Fd<math>\bar{3}</math>m</i>	5.65675			Ref 13
ORTHORHOMBIC_GA	(Ga)	<i>oS8</i>	<i>Cmca</i>	4.5197	7.6633	4.5260	Ref 14
HCP_A3	$\zeta$ -Ag <sub>2</sub> Ga	<i>hP2</i>	<i>P6<sub>3</sub>/mmc</i>	2.8818		4.6956	Ref 15
HCP_ORD	$\zeta'$ -Ag <sub>2</sub> Ga	<i>hP9</i>	<i>P6<math>\bar{2}</math>m</i>	7.7710		2.8788	Ref 15
AG3GA2	Ag <sub>3</sub> Ga <sub>2</sub>	...	<i>Pmmm</i>	6.7271	3.8764	3.1802	Ref 16

#### 3.1 Isothermal Section at 300 °C

For investigation of the phase equilibria at 300 °C, six samples were analyzed by EDS and XRD methods. Experimental results are summarized in Table 2.

Within six analyzed samples, five different phase regions were detected. Samples 1 and 2 have liquid, (Ge) and Ag<sub>3</sub>Ga<sub>2</sub> phases in the microstructure. Compositions of detected phases in both samples are close one to another. Liquid phase is rich in gallium, (Ge) solid solution phase with germanium and with neglected solubility of silver and gallium, while the intermetallic compound Ag<sub>3</sub>Ga<sub>2</sub> has composition close to the theoretical, with 60 at.% of silver and 40 at.% of gallium. Detected phases in the microstructure of the sample 3 are  $\zeta'$ , (Ge) and Ag<sub>3</sub>Ga<sub>2</sub>. Sample 4 has  $\zeta'$  and (Ge) as phase constituents.  $\zeta'$  phase is rich in silver (70.05 at.%), and 29.12 at.% of gallium, and neglected amount of germanium (0.83 at.%).

Sample 5 has  $\zeta'$ , (Ge), (Ag) phases in the microstructure. (Ag) and (Ge) solid solution phases have been identified within the sample 6. Solubility of silver and gallium in the (Ge) solid solution is negligible and solubility of gallium in (Ag) solid solution is 7.91 at.%.

EDS results, given in Table 2, are compared with calculated isothermal section at 300 °C (Fig. 2). In Fig. 1, overall compositions and compositions of coexisting phases determined by EDS analysis are labeled using the identical symbols in the same color.

Nine different phase regions are calculated for isothermal section at 300 °C. Two are single-phase regions [L and (Ag)], four are two-phase regions [L + (Ge), L + Ag<sub>3</sub>Ga<sub>2</sub>, (Ge) +  $\zeta'$  and (Ge) + (Ag)] and three are three-phase regions [L + (Ge) + Ag<sub>3</sub>Ga<sub>2</sub>, (Ge) +  $\zeta'$  + Ag<sub>3</sub>Ga<sub>2</sub> and (Ge) + (Ag) +  $\zeta'$ ]. Five of these nine phase regions are experimentally confirmed. By comparing experimental results and calculation, a good agreement has been reached.

SEM micrographs of two samples annealed at 300 °C are presented in Fig. 2 as an illustration.

Microstructure of sample 3 includes  $\zeta'$ , (Ge) and Ag<sub>3</sub>Ga<sub>2</sub> phases. (Ge) solid solution appears as a dark phase,  $\zeta'$  phase as a gray and Ag<sub>3</sub>Ga<sub>2</sub> compound as a light phase. Sample 6 includes (Ge) and (Ag) phases in the microstructure. As on micrographs of sample 3, (Ge) phase appears in microstructure of sample 6 as a dark phase, while (Ag) phase is a gray phase.

#### 3.2 Isothermal Section at 100 °C

As a next step, six alloys annealed at 100 °C were used for checking phase equilibria at 100 °C. Results of EDS and XRD analysis for the alloys annealed at 100 °C are summarized in Table 3.

**Table 2 EDS and XRD results of the ternary Ag-Ge-Ga samples annealed at 300 °C for four weeks**

No.	Composition of samples x, at.%	Determined phases		Compositions of phases x, at.%			Lattice parameters l (10 <sup>-10</sup> m)		
		EDS	XRD	Ag	Ge	Ga	a	b	c
1	Ag 11.19	L		13.45 ± 0.2	2.41 ± 0.3	84.14 ± 0.2			
	Ga 48.23	(Ge)	(Ge)	0.12 ± 0.3	99.79 ± 0.1	0.09 ± 0.4	5.6581(7)		
	Ge 40.58	Ag <sub>3</sub> Ga <sub>2</sub>	Ag <sub>3</sub> Ga <sub>2</sub>	58.94 ± 0.1	0.49 ± 0.5	40.57 ± 0.3	6.7198(5)	3.8751(7)	3.1792(5)
2	Ag 32.59	L		12.63 ± 0.7	3.18 ± 0.2	84.19 ± 0.1			
	Ga 38.26	(Ge)	(Ge)	0.13 ± 0.5	99.76 ± 0.1	0.11 ± 0.3	5.6601(3)		
	Ge 29.15	Ag <sub>3</sub> Ga <sub>2</sub>	Ag <sub>3</sub> Ga <sub>2</sub>	58.74 ± 0.2	1.50 ± 0.4	39.76 ± 0.2	6.7231(5)	3.8751(3)	3.1813(5)
3	Ag 56.27	ζ'	ζ'	65.74 ± 0.1	0.77 ± 0.6	33.49 ± 0.2	7.7531(5)		2.8752(1)
	Ga 33.07	(Ge)	(Ge)	0.09 ± 0.3	99.79 ± 0.1	0.12 ± 0.4	5.6573(2)		
	Ge 10.66	Ag <sub>3</sub> Ga <sub>2</sub>	Ag <sub>3</sub> Ga <sub>2</sub>	59.97 ± 0.5	1.45 ± 0.4	38.58 ± 0.4	6.7283(1)	3.8792(2)	3.1812(3)
4	Ag 55.64								
	Ga 23.05	ζ'	ζ'	70.05 ± 0.5	0.83 ± 0.3	29.12 ± 0.7	7.7222(3)		2.8855(3)
	Ge 21.31	(Ge)	(Ge)	0.09 ± 0.7	99.80 ± 0.1	0.11 ± 0.5	5.6563(2)		
5	Ag 66.15	ζ'	ζ'	74.79 ± 0.2	0.67 ± 0.1	24.54 ± 0.5	7.6834(5)		2.8831(5)
	Ga 16.51	(Ge)	(Ge)	0.07 ± 0.5	99.85 ± 0.1	0.08 ± 0.3	5.6568(3)		
	Ge 17.34	(Ag)	(Ag)	83.23 ± 0.7	1.24 ± 0.6	15.53 ± 0.3	4.1103(7)		
6	Ag 61.41								
	Ga 5.43	(Ge)	(Ge)	0.03 ± 0.1	99.9 ± 0.1	0.07 ± 0.1	5.6559(2)		
	Ge 33.16	(Ag)	(Ag)	89.61 ± 0.1	2.48 ± 0.2	7.91 ± 0.1	4.1090(4)		

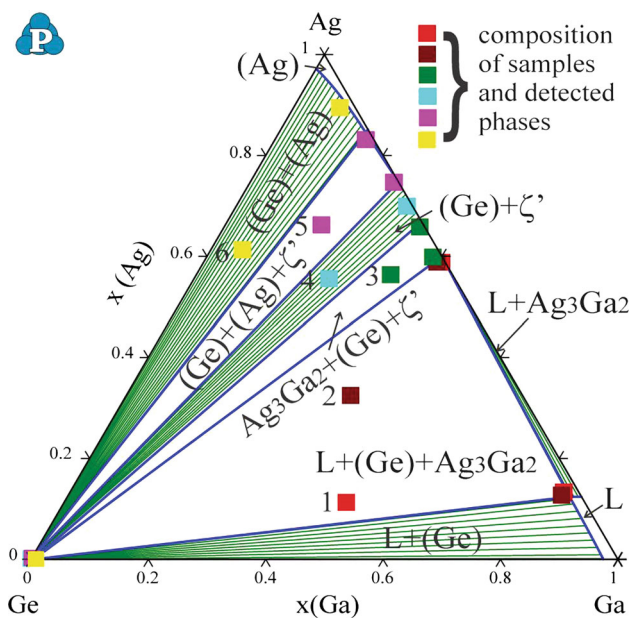


**Fig. 1** Predicted isothermal section at 300 °C compared with the EDS results of phase composition given in Table 2

Five different phase fields were identified: three three-phase regions [L + (Ge) + Ag<sub>3</sub>Ga<sub>2</sub>, ζ' + (Ge) + Ag<sub>3</sub>Ga<sub>2</sub> and ζ' + (Ge) + (Ag)] and two two-phase regions [ζ' + (Ge) and (Ge) + (Ag)]. The existence of L + (Ge) + Ag<sub>3</sub>Ga<sub>2</sub> three-phase region is confirmed by experimental results obtained for the samples 7 and 8. ζ' + (Ge) + Ag<sub>3</sub>Ga<sub>2</sub> three-phase region were identified by microstructural analysis of sample 9. Two-phase region ζ' + (Ge) is detected within the sample 10. Third three-phase region ζ' + (Ge) + (Ag) is detected within the sample 11. Sample 12 includes (Ge) and (Ag) as coexisting phases. Based on EDS results detected, liquid phase is rich in gallium, (Ge) solid solution is rich in germanium and can dissolve neglected

amount of silver and gallium, intermetallic compound Ag<sub>3</sub>Ga<sub>2</sub> have similar composition as theoretical, phase ζ' is rich in silver and gallium, and solid solution (Ag) is rich in silver and can dissolve more gallium than germanium. All experimental compositions of phases are compared with theoretical (calculated isothermal section at 100 °C) and presented in Fig. 3. Figure 3 presents calculated isothermal section at 100 °C, compared with EDS data given in Table 3, where overall compositions and compositions of coexisting phases are marked using the identical symbols and color.

Calculated isothermal section at 100 °C has five different phase regions. Calculated phase regions are the same as experimentally detected. By comparing EDS composition of phases with calculated composition, good agreement is visible.

Fig. 4 presents microstructures of samples 8 and 11.

### 3.3 Microstructural Analysis of Slowly Cooled Samples

Twelve slowly cooled ternary samples (marked with numbers from 13 to 24) were subjected to the tests of mechanical and electrical properties. Overall compositions of samples were situated along three vertical sections (samples 13 to 16, along Ag-GeGa vertical section, samples 17-20 along Ga-AgGe vertical section and samples from 21 to 24 along Ge-AgGa vertical section). Before determination of hardness and electrical conductivity, samples were analyzed using XRD and their microstructure was observed with light optical microscopy.

Results of XRD analysis of nine samples revealed that samples 13, 14, 18-24 have (Ga), (Ge) and Ag<sub>3</sub>Ga<sub>2</sub> phases in microstructure. Microstructure of the sample 15 includes (Ge) and ζ' phases. Sample 16 has (Ag), (Ge) and ζ' phases and sample 17 has Ag<sub>3</sub>Ga<sub>2</sub>, (Ge) and ζ' phases. Figure 5 presents calculated isothermal section at 25 °C with marked nominal composition of tested ternary alloys.

According to the calculation, samples marked with numbers 13, 14 and from 18 to 24 belong to the (Ga) + (Ge) + Ag<sub>3</sub>Ga<sub>2</sub> three-phase region, sample 15 belongs to the (Ge) + ζ' region, sample 16 to the (Ag) + (Ge) + ζ' region and sample 17 to the

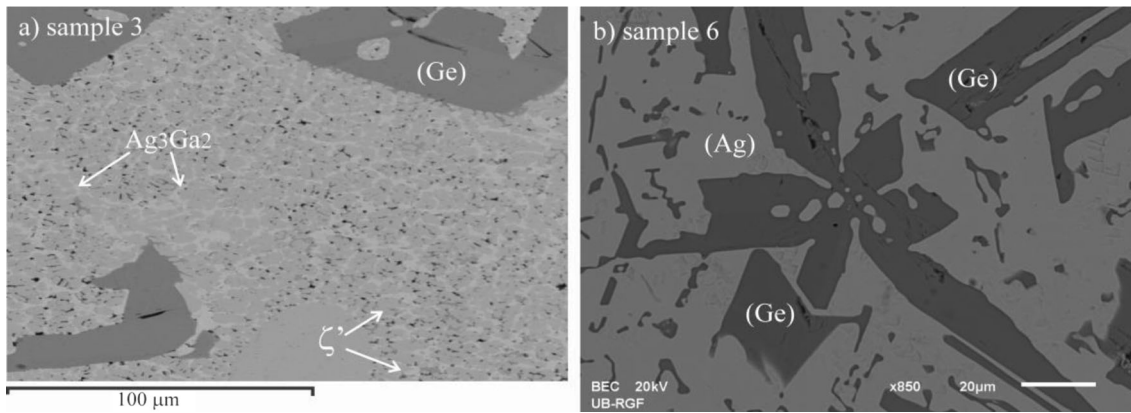


Fig. 2 SEM micrographs of (a) sample 3 and (b) sample 6

Table 3 EDS and XRD results of the ternary Ag-Ge-Ga samples annealed at 100 °C for six weeks

No.	Composition of samples x, at.%	Determined phases		Compositions of phases x, at.%			Lattice parameters l (10 <sup>-10</sup> m)		
		EDS	XRD	Ag	Ge	Ga	a	b	c
7	8.92 Ag	L		1.31 ± 0.3	0.55 ± 0.2	98.14 ± 0.2			
	72.22 Ga	(Ge)	(Ge)	0.09 ± 0.2	99.77 ± 0.4	0.14 ± 0.3	5.6573(3)		
8	18.86 Ge	Ag3Ga2	Ag3Ga2	58.94 ± 0.3	0.49 ± 0.4	40.57 ± 0.2	6.7183(4)	3.8744(3)	3.1775(3)
	28.68 Ag	L		1.10 ± 0.3	1.57 ± 0.5	97.33 ± 0.5			
9	33.95 Ga	(Ge)	(Ge)	0.60 ± 0.2	98.37 ± 0.5	1.03 ± 0.3	5.6569(5)		
	37.37 Ge	Ag3Ga2	Ag3Ga2	58.12 ± 0.1	1.08 ± 0.6	40.80 ± 0.4	6.7187(3)	3.8747(3)	3.1767(2)
10	43.09 Ag	ζ'	ζ'	65.53 ± 0.4	0.32 ± 0.6	34.15 ± 0.1	7.7521(8)		2.8743(5)
	25.28 Ga	(Ge)	(Ge)	0.40 ± 0.3	98.58 ± 0.2	1.02 ± 0.1	5.6573(5)		
11	31.63 Ge	Ag3Ga2	Ag3Ga2	60.18 ± 0.4	0.60 ± 0.4	39.22 ± 0.2	6.7248(2)	3.8738(1)	3.1787(2)
	52.77 Ag	ζ'	ζ'	69.44 ± 0.6	0.77 ± 0.3	29.79 ± 0.5	7.7213(5)		2.8832(1)
12	22.10 Ga	(Ge)	(Ge)	1.48 ± 0.5	97.47 ± 0.3	1.05 ± 0.3	5.6527(1)		
	25.13 Ge	ζ'	ζ'	74.59 ± 0.4	0.95 ± 0.2	24.46 ± 0.4	7.6815(2)		2.8811(3)
13	65.32 Ag	(Ge)	(Ge)	1.03 ± 0.2	97.30 ± 0.4	1.67 ± 0.3	5.6558(3)		
	9.56 Ga	(Ag)	(Ag)	88.38 ± 0.2	0.69 ± 0.1	10.93 ± 0.7	4.1073(8)		
14	25.12 Ge	(Ge)	(Ge)	1.30 ± 0.1	97.47 ± 0.5	1.30 ± 0.2	5.6538(1)		
	72.32 Ag	(Ag)	(Ag)	95.37 ± 0.3	0.52 ± 0.3	4.11 ± 0.1	4.0893(1)		

Ag<sub>3</sub>Ga<sub>2</sub> + (Ge) + ζ' region. By comparing XRD results and calculation, same phase regions are calculated and experimentally determined. Further, these samples were used for measurements of mechanical and electrical properties. Four microstructures of samples 13, 15, 17 and 22 are given in Fig. 6.

Phases which appear in microstructures are marked at presented micrographs.

### 3.4 Brinell Hardness Measurements

Twelve ternary samples and three binary samples were subjected to the Brinell hardness measurements. Three measurements were performed for each sample. Based on repeated measurements, mean values of Brinell hardness were calculated and presented in Table 4. Table 4 also shows overall compositions and phase fractions of the investigated alloys. Phase fractions of all investigated alloys at room temperature were calculated using thermodynamic database. Phase fractions for the samples 13, 15, 17 and 22 were also estimated by image

analysis of the optical micrographs (Fig. 6) for comparison. From the data given in Table 4, it can be seen that there is relatively good agreement between calculated phase fractions and phase fractions estimated by image analysis for the samples 13 and 22. In the case of sample 15, thermodynamic calculations indicate three phases [(Ge), (Ag), ζ'] in equilibrium at room temperature, while the experimental results of metallographic and XRD analysis point out to the coexistence of two phases [(Ge) and ζ']. Similarly, for the sample 17, two phases ((Ge) and ζ') were predicted by thermodynamic calculation and three phases [(Ge), ζ', Ag<sub>3</sub>Ga<sub>2</sub>] were experimentally observed. The reason for these disagreements could be small deviations of samples' overall compositions from their initial (designed) compositions. According to the calculated phase diagram of the Ag-Ge-Ga given in Fig. 5, initial overall compositions of samples 15 and 17 are very close to the phase borders between corresponding two-phase and three-phase fields. The literature values of hardness for pure elements (Ref 17) are also shown in Table 4 for comparison.

Based on the obtained results given in Table 4, it can be seen that Ge-rich samples 23 and 24 have a very high values of Brinell hardness. Their microstructures are based on (Ge) solid solution phase and  $\text{Ag}_3\text{Ga}_2$  intermetallic phase with very small phase fraction of (Ga) phase. Among all investigated alloys, the highest value of Brinell hardness is identified for the sample 15 with high content of Ag. Although pure Ag has very small hardness, high value of hardness for sample 15 is probably caused by a very large phase fraction (0.74) of  $\zeta'$  intermetallic compound (see Fig. 6b). The lowest values of Brinell hardness were determined for the Ga-rich samples 19 and 20. Their microstructure consists of (Ga), (Ge) and  $\text{Ag}_3\text{Ga}_2$  phases with very high phase fractions of (Ga) phase. It can be concluded that increase in (Ge) and  $\zeta'$  phase fractions increases alloy hardness, while increase in (Ga) phase fraction leads to decrease in alloy hardness.

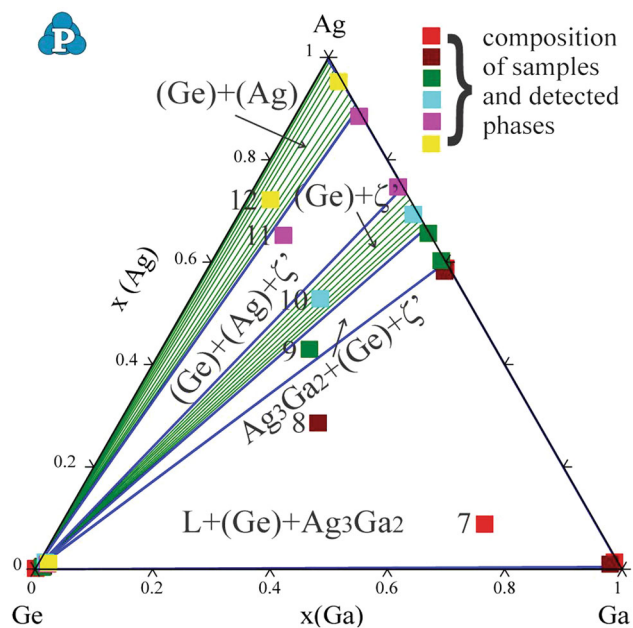


**Fig. 3** Predicted isothermal section at 100 °C compared with the EDS results of phase composition given in Table 3

### 3.5 Electrical Conductivity Measurements

The same twelve ternary samples and three binary samples that were used for hardness measurements were used for determination of electrical conductivity. Electrical conductivity measurements for each sample were performed in four points and obtained results are summarized in Table 5, together with the literature values of electrical conductivity for pure constitutive elements (Ref 18).

As it is expected, chemical composition of the alloys has strong effect on electrical conductivity. As it is expected, electrical conductivity generally increases with an increase in silver amount. From the studied ternary samples with compositions along the cross section with equal molar fractions of Ga and Ge, the highest electrical conductivity is obtained for the alloy 16, with the highest amount of Ag. However, positive correlation between alloy content of Ag and alloy electrical

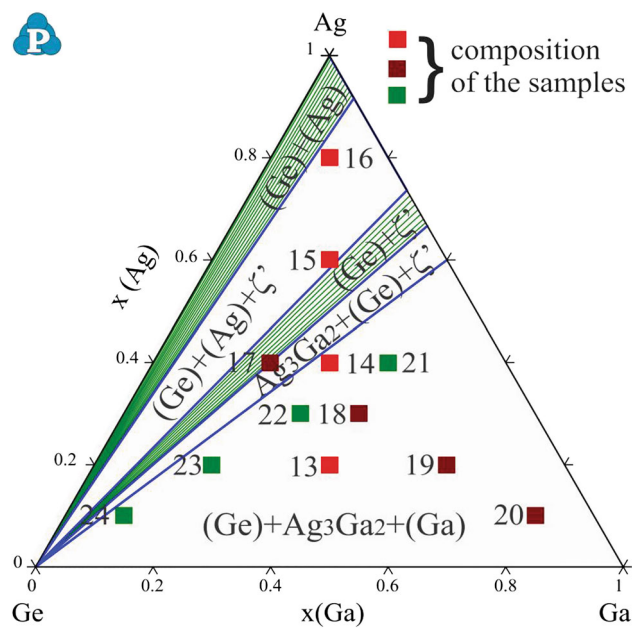


**Fig. 5** Predicted isothermal section at 25 °C with marked compositions of tested alloys

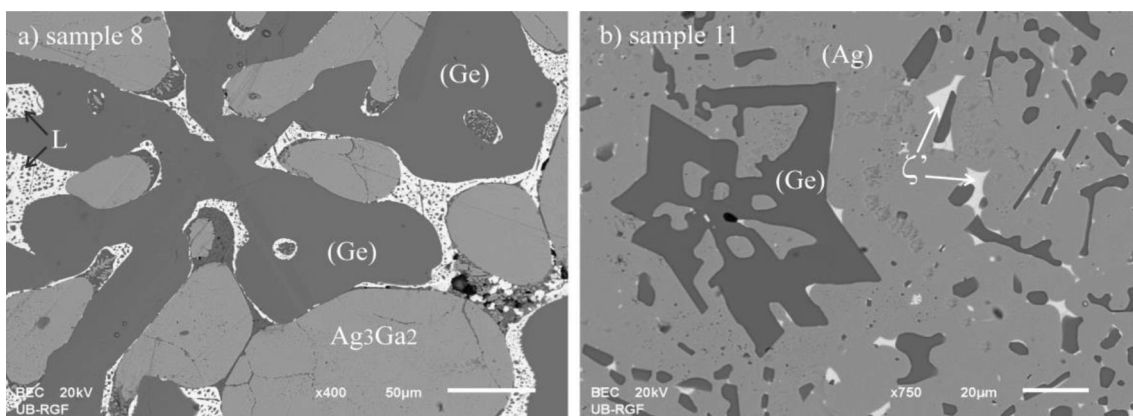


**Fig. 4** SEM micrographs of (a) sample 8 and (b) sample 11

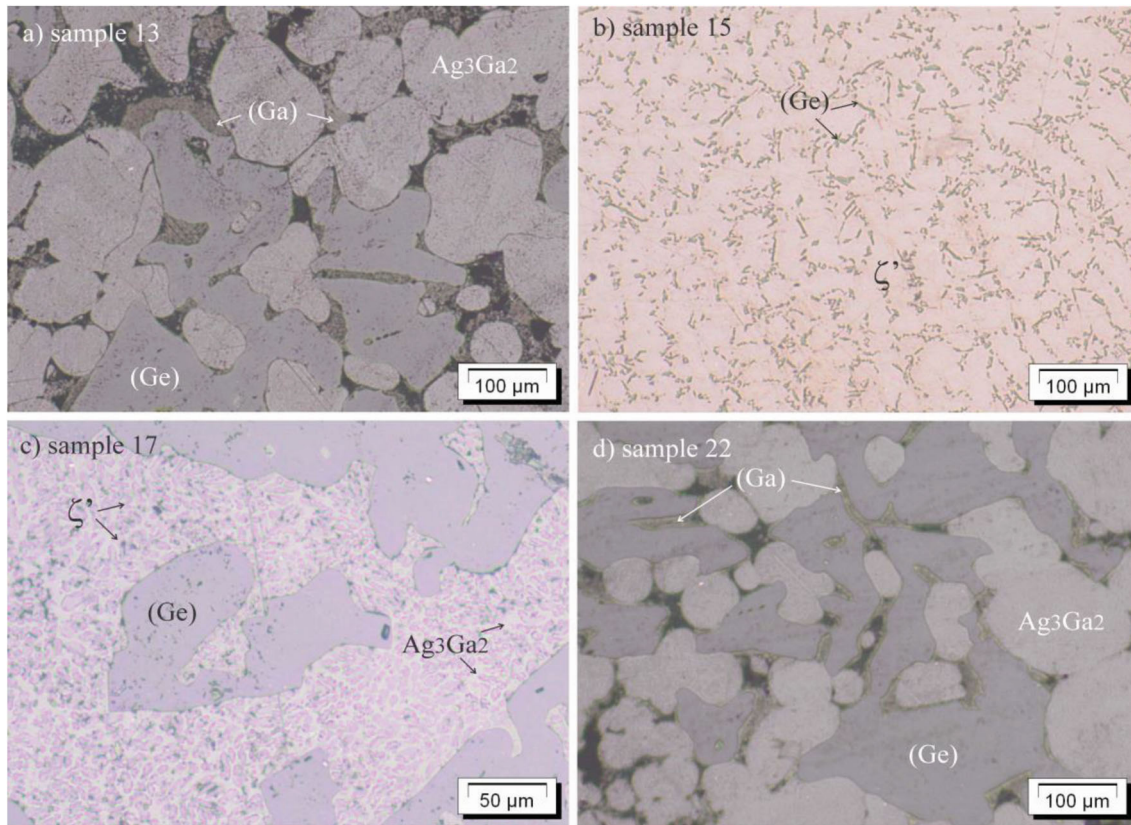


Fig. 6 LOM micrographs of: (a) sample 13, (b) sample 15, (c) sample 17 and (d) sample 22

Table 4 Compositions of the investigated samples with calculated phase fractions at room temperature and related Brinell hardness values

No.	Alloy nominal composition, at.%	Calculated fraction of a phase, %	Fraction of a phase determined by image analysis, %	Measured value, MN/m <sup>2</sup>			Mean value, MN/m <sup>2</sup>
				1	2	3	
B1	Ga <sub>50</sub> Ge <sub>50</sub>	50%(Ga), 50%(Ge)		106	102.4	121.6	110
13	Ag <sub>20</sub> Ga <sub>40</sub> Ge <sub>40</sub>	27%(Ga), 33%Ag <sub>3</sub> Ga <sub>2</sub> , 40%(Ge)	22%(Ga), 36%Ag <sub>3</sub> Ga <sub>2</sub> , 42%(Ge)	31.1	37.3	45.3	37.9
14	Ag <sub>40</sub> Ga <sub>30</sub> Ge <sub>30</sub>	3%(Ga), 67%Ag <sub>3</sub> Ga <sub>2</sub> , 30%(Ge)		71.6	68.0	86.6	75.4
15	Ag <sub>60</sub> Ga <sub>20</sub> Ge <sub>20</sub>	20%(Ge), 6%(Ag), 74%ζ'	14%(Ge), 86%ζ'	226.4	324.3	249.2	266.6
16	Ag <sub>80</sub> Ga <sub>10</sub> Ge <sub>10</sub>	10%(Ge), 76%(Ag), 14%ζ'		134.2	123.4	129.6	129.1
	Ag	100%Ag					24.5
B2	Ag <sub>50</sub> Ge <sub>50</sub>	50%(Ag), 50%(Ge)		94.8	89.6	93.4	92.6
17	Ag <sub>40</sub> Ga <sub>20</sub> Ge <sub>40</sub>	40%(Ge), 60%ζ'	44%(Ge), 38%ζ', 18%Ag <sub>3</sub> Ga <sub>2</sub>	165.5	145.2	113.6	141.4
18	Ag <sub>30</sub> Ga <sub>40</sub> Ge <sub>30</sub>	30%(Ge), 50%Ag <sub>3</sub> Ga <sub>2</sub> , 20%(Ga)		90.7	80.2	88.6	86.5
19	Ag <sub>20</sub> Ga <sub>60</sub> Ge <sub>20</sub>	20%(Ge), 47%(Ga), 33%Ag <sub>3</sub> Ga <sub>2</sub> ,		29.3	25.0	28.1	27.46
20	Ag <sub>10</sub> Ga <sub>80</sub> Ge <sub>10</sub>	10%(Ge), 17%Ag <sub>3</sub> Ga <sub>2</sub> , 73%(Ga)		23.7	23.2	23.4	23.43
	Ga	100%Ga					60
B3	Ag <sub>50</sub> Ga <sub>50</sub>	83%Ag <sub>3</sub> Ga <sub>2</sub> , 17%(Ga)		77.6	68.4	78.4	74.8
21	Ag <sub>40</sub> Ga <sub>40</sub> Ge <sub>20</sub>	20%(Ge), 67%Ag <sub>3</sub> Ga <sub>2</sub> , 13%(Ga)		68.6	71.3	63.8	67.9
22	Ag <sub>30</sub> Ga <sub>30</sub> Ge <sub>40</sub>	40%(Ge), 50%Ag <sub>3</sub> Ga <sub>2</sub> , 10%(Ga)	45%(Ge), 42%Ag <sub>3</sub> Ga <sub>2</sub> , 13%(Ga)	126.4	142.1	138.6	135.7
23	Ag <sub>20</sub> Ga <sub>20</sub> Ge <sub>60</sub>	40%(Ge), 6%(Ga), 33%Ag <sub>3</sub> Ga <sub>2</sub>		244.6	230.5	238.6	237.9
24	Ag <sub>10</sub> Ga <sub>10</sub> Ge <sub>80</sub>	80%(Ge), 3%(Ga), 17%Ag <sub>3</sub> Ga <sub>2</sub>		230.5	213.8	193.4	212.5
	Ge	100%Ge					366.74

conductivity is not very strong, which leads to the conclusion that beside alloy composition, phase constituents and their amounts also have significant influence on electrical conductivity (Ref 19).

#### 4. Conclusions

In this study, two isothermal sections at 100 and 300 °C of the ternary Ag-Ge-Ga system were experimentally investigated

**Table 5** Compositions of the investigated samples with calculated phase fractions at room temperature and related electrical conductivity values

No.	Alloy nominal composition, at. %	Calculated fraction of a phase, %	Fraction of a phase determined by image analysis, %	Value (MS /m)				Mean value, MS/m
				1	2	3	4	
B1	Ga <sub>50</sub> Ge <sub>50</sub>	50%(Ga), 50%(Ge)		1.812	1.767	1.641	1.412	1.658
13	Ag <sub>20</sub> Ga <sub>40</sub> Ge <sub>40</sub>	27%(Ga), 33%Ag <sub>3</sub> Ga <sub>2</sub> , 40%(Ge)	22%(Ga), 36%Ag <sub>3</sub> Ga <sub>2</sub> , 42%(Ge)	5.824	5.723	5.877	5.768	5.798
14	Ag <sub>40</sub> Ga <sub>30</sub> Ge <sub>30</sub>	3%(Ga), 67%Ag <sub>3</sub> Ga <sub>2</sub> , 30%(Ge)		2.511	2.509	2.561	2.528	2.527
15	Ag <sub>60</sub> Ga <sub>20</sub> Ge <sub>20</sub>	20%(Ge), 6%(Ag), 74%ζ'	14%(Ge), 86%ζ'	4.26	4.396	4.302	4.346	4.326
16	Ag <sub>80</sub> Ga <sub>10</sub> Ge <sub>10</sub>	10%(Ge), 76%(Ag), 14%ζ' Ag		8.776	8.776	8.824	8.812	8.797
B2	Ag <sub>50</sub> Ge <sub>50</sub>	50%(Ag), 50%(Ge)		9.862	11.064	10.104	10.026	10.264
17	Ag <sub>40</sub> Ga <sub>20</sub> Ge <sub>40</sub>	40%(Ge), 60%ζ'	44%(Ge), 38%ζ', 18%Ag <sub>3</sub> Ga <sub>2</sub>	2.103	2.098	2.122	2.083	2.102
18	Ag <sub>30</sub> Ga <sub>40</sub> Ge <sub>30</sub>	30%(Ge), 50%Ag <sub>3</sub> Ga <sub>2</sub> , 20%(Ga)		6.706	6.768	6.742	6.684	6.725
19	Ag <sub>20</sub> Ga <sub>60</sub> Ge <sub>20</sub>	20%(Ge), 47%(Ga), 33%Ag <sub>3</sub> Ga <sub>2</sub> ,		3.585	3.338	3.357	3.464	3.436
20	Ag <sub>10</sub> Ga <sub>80</sub> Ge <sub>10</sub>	10%(Ge), 17%Ag <sub>3</sub> Ga <sub>2</sub> , 73%(Ga) Ga		4.332	4.298	4.283	4.274	4.297
B3	Ag <sub>50</sub> Ga <sub>50</sub>	83%Ag <sub>3</sub> Ga <sub>2</sub> , 17%(Ga)		13.708	13.568	12.986	13.486	13.437
21	Ag <sub>40</sub> Ga <sub>40</sub> Ge <sub>20</sub>	20%(Ge), 67%Ag <sub>3</sub> Ga <sub>2</sub> , 13%(Ga)		3.579	3.559	3.557	3.584	3.57
22	Ag <sub>30</sub> Ga <sub>30</sub> Ge <sub>40</sub>	40%(Ge), 50%Ag <sub>3</sub> Ga <sub>2</sub> , 10%(Ga)	45%(Ge), 42%Ag <sub>3</sub> Ga <sub>2</sub> , 13%(Ga)	5.954	6.324	6.248	6.306	6.208
23	Ag <sub>20</sub> Ga <sub>20</sub> Ge <sub>60</sub>	40%(Ge), 6%(Ga), 33%Ag <sub>3</sub> Ga <sub>2</sub>		1.068	1.060	1.055	1.063	1.062
24	Ag <sub>10</sub> Ga <sub>10</sub> Ge <sub>80</sub>	80%(Ge), 3%(Ga), 17%Ag <sub>3</sub> Ga <sub>2</sub> Ge		0.6036	0.601	0.5999	0.6026	0.602
		100%Ge						1.344

and thermodynamically extrapolated. SEM-EDS and XRD analysis were applied for microstructural analysis of the chosen ternary sample after long-term annealing. Experimentally determined compositions of coexisting phases were in good agreement with related calculated compositions. Conducted experiments did not indicate any new ternary phases or large solubility of third element in binary phases. Optical microscopy and XRD analysis together with the hardness and electrical conductivity measurements were performed on three binary and twelve slowly cooled ternary alloys. Experimentally determined phases by XRD analysis were compared with calculated isothermal section at 25 °C and agreement between the results was reached. Results of Brinell hardness and electrical conductivity measurements were presented and discussed with respect to alloy compositions and phase constituents.

## Acknowledgments

This work has been supported by the Ministry of Education, Science and Technological Development of the Republic of Serbia (Grant No. OI172037).

## References

1. D. Milisavljević, D. Minić, M. Premović, D. Manasijević, and L. Balanović, Experimental Examination and Thermodynamic Description of the Ternary Ag-Ge-Ga System, *J. Phys. Chem. Solids*, 2019, **126**, p 55–64
2. J. Wang, Y.J. Liu, C.Y. Tang, L.B. Liu, H.Y. Zhou, and Z.P. Jin, Thermodynamic Description of the Au-Ag-Ge Ternary System, *Thermochim. Acta*, 2011, **512**, p 240–246
3. W. Gierlotka and D. Jendrzeczyk-Handzlik, Thermodynamic Description of the Binary Ag-Ga System, *J. Alloy. Compd.*, 2011, **509**(1), p 38–42
4. I. Ansara, J.P. Bros, and M. Gambino, Thermodynamic Analysis of the Germanium-Based Ternary Systems Al-Ga-Ge, Al-Ge-Sn, Ga-Ge-Sn, *Calphad*, 1979, **3**, p 225–233
5. W. Cao, S.L. Chen, F. Zhang, K. Wu, Y. Yang, Y.A. Chang, R. Schmid-Fetzer, and W.A. Oates, PANDAT Software with Panengine, Panoptimizer and Panprecipitation for Multicomponent Phase Diagram Calculation and Materials Property Simulation, *Calphad*, 2009, **33**(2), p 328–342
6. H. Kazemi and L. Weber, Solid Solubility of Germanium in Silver, *Thermochim. Acta*, 2012, **544**, p 57–62
7. Z.H. Long, S.X. Zhou, H.S. Liu, and Z.P. Jin, Thermodynamic Assessment of Ag-Dy-Sb Ternary System, *Thermochim. Acta.*, 2010, **498**, p 22–26
8. M. Premovic, D. Manasijevic, D. Minic, and D. Zivkovic, Experimental Investigation and Thermodynamic Prediction of the Ag-Ge-Sb Phase Diagram, *J. Alloy. Compd.*, 2014, **610**, p 161–168
9. S. Raoux and T.J. Ibm, Phase Change Memory (PCM) Materials and Devices, *Advances in Nonvolatile Memory and Storage Technology*, 2nd ed., Y. Nishi, Ed., Elsevier, Amsterdam, 2014, p 161–199
10. T. Siegrist, P. Jost, H. Volker, M. Woda, P. Merkelbach, C. Schlockermann, and M. Wuttig, Disorder-Induced Localization in Crystalline Phase-Change Materials, *Nat. Mater.*, 2011, **10**, p 202–208
11. N. Yamada, E. Ohno, N. Akahira, K. Nishiuchi, K. Nagata, and M. Takao, High Speed Over Writable Phase Change Optical Disk Material, *Jpn. J. Appl. Phys.*, 1987, **26**, p 61–66
12. E. Jette and F. Foote, Precision Determination of Lattice Constants, *J. Chem. Phys.*, 1935, **3**, p 605–616
13. A.S. Cooper, Precise Lattice Constants of Germanium, Aluminum, Gallium Arsenide, Uranium, Sulphur, Quartz and Sapphire, *J. Appl. Phys.*, 1983, **54**, p 3609–3611
14. B.D. Sharma and J. Donohue, A Refinement of the Crystal Structure of Gallium Cryst, *Adv. Mater.*, 1962, **117**, p 293–300
15. Y. Zhang, Q.L. Liu, J.B. Li, J.K. Liang, J. Luo, F.S. Liu, Y.G. Xiao, and G.H. Rao, Structure of the Zeta-Phase and Zeta'-Phases in the Ag-Ga System, *J. Alloys Compd.*, 2005, **399**, p 155–159
16. D. Minić, M. Premović, D. Manasijević, V. Čosović, D. Zivković, and A. Marković, Experimental Investigation and Thermodynamic Calculations of the Ag-Bi-Ga Phase Diagram, *J. Alloys Compd.*, 2015, **646**, p 461–471

17. <http://periodictable.com/Properties/A/BrinellHardness.al.html>. Accessed 29 Nov 2018
18. <http://periodictable.com/Properties/A/ElectricalConductivity.an.html>. Accessed 30 Nov 2018
19. C. Zhang, Y. Du, S. Liu, Y. Liu, and B. Sundman, Thermal Conductivity of Al-Cu-Mg-Si Alloys: Experimental Measurement

and CALPHAD Modeling, *Thermochim. Acta.*, 2016, **635**, p 8–16

**Publisher's Note** Springer Nature remains neutral with regard to jurisdictional claims in published maps and institutional affiliations.